Global Methods for Compressive Sensing in MIMO Radar with Distributed Sensors

Marco Rossi$^{(*)}$, Alexander M. Haimovich$^{(*)}$, and Yonina C. Eldar$^{(\dagger)}$
$^{(*)}$CWCSPR, New Jersey Institute of Technology, Newark, NJ07102-1982, USA
$^{(\dagger)}$Department of EE Technion, Israel Institute of Technology, Haifa 32000, Israel
Email: {marco.rossi, alexander.m.haimovich}@njit.edu, yonina@ee.technion.ac.il

***Abstract*— We study compressive sensing methods for target localization in MIMO radar. While much attention has been given to compressive sensing of signal measurements in the time domain, this work focuses on the spatial domain. We propose a framework in which the target localization with distributed, active sensors is formulated as a nonconvex optimization. By leveraging a sparse representation, we devise a branch-and-bound type algorithm that provides a global solution to the nonconvex localization problem. It is shown that this method can achieve high resolution target localization with a highly undersampled MIMO radar with transmit/receive elements placed at random. A lower bound is developed on the number of transmit/receive elements required to ensure accurate target localization with high probability.**

I. Introduction

Basic functions of a radar are detection, estimation, and tracking of targets. In multiple input multiple output (MIMO) radar [1], targets are probed with multiple, simultaneous waveforms. Returns from the targets are jointly processed relying on multiple receive antennas and the properties of the transmitted waveforms. Depending on the mode of operation and system architecture, MIMO radars have been shown to boost target detection, enhance spatial resolution, and improve interference suppression. MIMO radars achieve these advantages by exploiting a larger number of degrees of freedom than "conventional" radar and possibly the target's spatial diversity. In this work, we focus on the application of MIMO radar to the estimation of direction-of-arrival (DOA).

It is well known in array processing that resolution improves with the array aperture. A non-ambiguous uniform linear array (ULA) must have its elements spaced at intervals no larger than $\lambda/2$. For a MIMO radar, unambiguous direction finding of targets is possible for $\lambda/2$-spaced receive elements and $N\lambda/2$-spaced transmit elements (a virtual filled array), where N is the number of receive elements [2]. Thus for both passive and active direction finding, the number of sensors increases linearly with the array aperture, therefore with the required resolution. To benefit from the advantages, but avoid the costs, of a large aperture, various ways were proposed to thin the number of elements of a phased array. With random arrays, a relatively low number of elements are randomly placed across a large aperture. Studies of random arrays have shown that the probability of a sidelobe competing with the mainlobe decreases with the number of array elements. Moreover, a threshold phenomena has been demonstrated: below a threshold number of sensors, the probability of a peak sidelobe is high, while above the threshold, the probability of a peak sidelobe is very low [3]. More recently, the concept of random array has been extended to MIMO radar [4] employing the beamforming estimator and assuming only 1 target is present. Under this scenario, it is shown that in a M tx and N rx MIMO radar. system, it is possible to obtain the same sidelobe performance as a system with 1 transmitter and MN receive elements, delivering savings for $M+N<MN$.

The $\lambda/2$-spaced array and the MIMO virtual filled array perform spatial sampling at Nyquist rate, while the random array and the MIMO random array sample the space at sub-Nyquist rates. Recovering targets from undersampled array data, links random arrays to the *compressed sensing* (CS) paradigm. In CS, one seeks to recover a K-*sparse* vector $\mathbf{x}$ of length G, $K \ll G$ from MN non-adaptive, linear observations of the form of $\mathbf{y}=\mathbf{A}\mathbf{x}$, where the $MN \times G$ matrix $\mathbf{A}$, with $MN \ll G$, is commonly referred to as *dictionary*, and its columns are called *atoms*.. The unknown vector $\mathbf{x}$ carries information on the location and strength of the K targets. The idea is to recast the inverse problem (i.e., determining the target location from sensors observations) in an optimization framework, where the (known) columns of $\mathbf{A}$ are the steering vectors from a grid of possible targets locations. While the system $\mathbf{y}=\mathbf{A}\mathbf{x}$ is highly underdetermined, finding conditions that guarantee correct recovery when the unknown vector $\mathbf{x}$ is sparse, has been a main topic of research and one of the underpinnings of CS theory. In this regard, linear independence of subset of columns of the matrix $\mathbf{A}$ play a key role: while each column of the matrix for a filled ULA has Vandermonde structure (ensuring *any* MN set of columns being linearly independent), intuitively, the chance of having dependent columns of $\mathbf{A}$ increases as the number of sensors is thinned and the Vandermonde structure abandoned. Exploring relations between the number of rows and columns of $\mathbf{A}$ and the number of targets is a main topic of this paper.

In the MIMO radar application, of great interest are solutions that require the least amount of sensors to guarantee correct recovery of the unknown targets. One way to achieve this goal is to globally solve the non-convex combinatorial ℓ_0-norm problem (i.e., $\min \|\mathbf{x}\|_0$ subject to $\mathbf{y}=\mathbf{A}\mathbf{x}$). Unfortunately, in general, its solution comes at the cost of an exponential complexity exhaustive search [5]. Two main suboptimal approaches can be found in the literature: greedy algorithms, such as Orthogonal Least Squares (OLS) [6], and relaxing the ℓ_0-norm to an ℓ_1-norm, resulting in a convex problem [7]. Moreover, it has been recently shown that the non-convex problem where the ℓ_0-norm is replaced with a proper *concave* sparsity enforcing $f(|\mathbf{x}|)$, can recover $\mathbf{x}$ with fewer measurements then needed by relaxing the ℓ_0-norm to the convex ℓ_1-norm [8]. This motivates the design of high performance algorithms that can perform well with a low number of transmit and receive elements.

Recent work on CS includes applications to radar, with the focus on time sampling [9], [10], [11], [15] and to MIMO radar [**?**]. In this paper, we are interested mainly in spatial CS using a random array geometry, as opposed to the ULA [12] and virtual ULA [13] geometries. Links between CS and random arrays are explored in [14] for the passive DOA problem. Concerning random arrays for MIMO radar, in [16], a CS algorithm known as the Dantzig selector, is used to extract angle and Doppler information with randomly located sensors. The authors show that the correlation between columns of the matrix $\mathbf{A}$ decreases with the number of sensors, and, by applying standard CS results, they obtain a lower bound on the number of sensors needed for correct recovery. However, this bound increases linearly with the mutual coherence of $\mathbf{A}$, precluding high resolution with a small number of elements.

The work presented in this paper goes beyond the scope of the reviewed literature, and makes the following contributions:

1) Develop a global, branch-and-bound (BB) algorithm for the sparse recovery problem that extend the OLS idea.

2) Derive an explicit lower bound on MN for OLS algorithm's correct recovery, and show that it is proportional to the number of targets K and logarithmically proportional to the array aperture. This provides specific insight into links between random arrays and CS algorithms, and demonstrates that a high resolution can be obtained with a relatively low number of randomly placed sensors.

The following notations are used. The boldface denotes matrices (uppercase) and vectors (lowercase); $(\cdot)^*$ denotes the complex conjugate operator, $(\cdot)^T$ denotes the transpose operator, $(\cdot)^H$ is the complex conjugate-transpose operator, and $(\cdot)^\dagger$ is the pseudo-inverse. The symbol "$\otimes$" denotes the Kronecker product. Finally, given a set S of indices, $|S|$ denotes its cardinality, $\mathbf{A}_S$ is the sub-matrix obtained by considering only the columns indexed in S, and we define the projection matrix $\Pi^{\perp}_{\mathbf{A}_S} \triangleq \mathbf{I} - \mathbf{A}_S\mathbf{A}_S^{\dagger}$.

II. Problem Formulation

We model a MIMO radar system where N sensors collect the signals transmitted by M transmitters and returned from K stationary targets. We assume that transmitters and receivers each form a (possibly overlapping) linear array of total aperture Z_T and Z_R, respectively: the m-th transmitter is at position ξ_m on the x-axis, while n-th receiver is at position ζ_n (with $\xi_m \in [0, Z_T]\ \ \forall m$ and $\zeta_n \in [0, Z_R]\ \forall n$). Targets are assumed in the far-field, meaning that a target's aspect angle θ_k is constant across the array. The purpose of the system is to determine the DOA angles to the targets. The $N \times L$ matrix representing the sampled received signal is

$$\mathbf{Y} = \sum_{k=1}^{K} x_k \mathbf{b}\left(\theta_k\right) \mathbf{c}^T\left(\theta_k\right) \mathbf{S} + \mathbf{N} \tag{1}$$

where x_k is the k-th target's response, the $N \times 1$ vector $\mathbf{b}\left(\theta_k\right) = \frac{1}{\sqrt{N}}\left[\exp\left(j2\pi\frac{\sin\theta_k}{\lambda}\zeta_1\right), \ldots, \exp\left(j2\pi\frac{\sin\theta_k}{\lambda}\zeta_N\right)\right]^T$ accounts for the angular response between the k-th target and each receiver sensor, the $M \times 1$ vector $\mathbf{c}\left(\theta_k\right) = \frac{1}{\sqrt{M}}\left[\exp\left(j2\pi\frac{\sin\theta_k}{\lambda}\xi_1\right), \ldots, \exp\left(j2\pi\frac{\sin\theta_k}{\lambda}\xi_M\right)\right]^T$ accounts for the angular response between the k-th target and each transmitter, and the $M \times L$ matrix $\mathbf{S}$ contains the L samples of the M signals transmitted by the MIMO radar. We assume the M transmitted signals to be orthogonal (e.g., waveforms coded by an orthogonal code). Finally, the $N \times L$ matrix $\mathbf{N}$ models the noise (assumed temporally and spatially white).

By vectorizing the outputs of all the receivers' matched filters (i.e., $\mathbf{y} \triangleq \frac{M}{L}\left(\mathbf{S}^* \otimes \mathbf{I}_N\right)\mathrm{vec}\left[\mathbf{Y}\right]$), we obtain

$$\mathbf{y} = \tilde{\mathbf{A}}\left(\boldsymbol{\theta}\right)\tilde{\mathbf{x}} + \mathbf{n} \tag{2}$$

where $\mathbf{y}$ is $MN \times 1$, $\tilde{\mathbf{x}} = \left[x_1, \ldots, x_K\right]^T$, $\tilde{\mathbf{A}}\left(\boldsymbol{\theta}\right) = \left[\mathbf{c}\left(\theta_1\right) \otimes \mathbf{b}\left(\theta_1\right), \ldots, \mathbf{c}\left(\theta_K\right) \otimes \mathbf{b}\left(\theta_K\right)\right]$ and $\mathbf{n} \triangleq \frac{M}{L}\left(\mathbf{S}^* \otimes \mathbf{I}_N\right)\mathrm{vec}\left[\mathbf{N}\right]$. To embed the DOA estimation into a sparse localization framework, we discretize the possible targets' locations $\boldsymbol{\theta}$, obtaining a grid of G points $\left\{\phi_g\right\}$ (with $G \gg K$). Defining the $MN \times G$ matrix $\mathbf{A} = \left[\mathbf{a}\left(\phi_1\right), \ldots, \mathbf{a}\left(\phi_G\right)\right]$ where $\mathbf{a}\left(\theta\right) \triangleq \mathbf{c}\left(\theta\right) \otimes \mathbf{b}\left(\theta\right)$, the localization problem is expressed in the CS framework:

$$\mathbf{y} = \mathbf{A}\mathbf{x} + \mathbf{n} \tag{3}$$

where the unknown $G \times 1$ vector $\mathbf{x}$ contains the targets location and gains. Zero elements of $\mathbf{x}$ correspond to grid points without a target. The problem (3) is sparse in the sense that the support of $\mathbf{x}$ should have only $K \ll G$ elements. Moreover, we are interested in solutions that require a relatively small number of transmitters and receivers. Lower bounds on the number of array elements are discussed in the next section.

III. Lower bounds on the number of sensors

The problem (3) is the sparse recovery of target directions and gains from a single measurement vector (SMV) of sub-Nyquist spatial samples. In this section, we establish a lower bound on the number of random elements of a MIMO radar system. The bound is customized to the OLS algorithm, and it guarantees correct recovery with high probability. Throughout this section, we make the simplifying assumptions that targets are located on grid points, and measurements are noiseless. Using standard CS arguments, $MN \geq 2K$ is a necessary and sufficient condition for the global solution to the non-convex ℓ_0 problem to recover the original K DOAs. Unfortunately, solving the ℓ_0 problem requires an exhaustive search over all K-sparse vectors, at the cost of exponential complexity.

A suboptimal approach to reduce complexity is by *greedy* search strategies, of which the OLS algorithm is one example. The algorithm works by computing location and gain, one target at a time. For example, given a target found at angle θ_1, the observations vector $\mathbf{y}$ is projected onto the null-space of the steering vector $\mathbf{a}(\theta_1)$ via the projection matrix $\Pi^{\perp}_{\mathbf{a}(\theta_1)}$. Similarly, the columns of the matrix $\mathbf{A}$ are projected onto the null-space of $\mathbf{a}(\theta_1)$ and then renormalized. The method proceeds to estimate iteratively each of the remaining targets with the new residual and the new dictionary. For the estimation of the first target to be successful, it is required that

$$\frac{\max_{\phi_g \notin \boldsymbol{\theta}} \left|\mathbf{y}^H \mathbf{a}\left(\phi_g\right)\right|}{\max_{\phi_g \in \boldsymbol{\theta}} \left|\mathbf{y}^H \mathbf{a}\left(\phi_g\right)\right|} < 1 \tag{4}$$

where ϕ_g, $g = 1, \ldots, G$ are the directions associated with the grid, and $\boldsymbol{\theta} = \{\theta_k\}_{k=1}^K$ is the set of target locations. The numerator $\max_{\phi_g \notin \boldsymbol{\theta}} \left|\mathbf{y}^H \mathbf{a}\left(\phi_g\right)\right|$ is the maximum response of the array beamformed at ϕ_g for grid points without targets. In phased array parlance, this is the *peak sidelobe*. Noting that the noiseless snapshot across the array is given by $\mathbf{y} = \sum_{k=1}^K \mathbf{a}(\theta_k) x_k$, correct estimation of the first target is guaranteed if the peak sidelobe $< \max_k \left(|x_k| - \left|\sum_{j\neq k} x_j \mathbf{a}^H(\theta_j)\mathbf{a}(\theta_k)\right|\right) \leq \max_{\phi_g \in \boldsymbol{\theta}} \left|\mathbf{y}^H \mathbf{a}\left(\phi_g\right)\right|$.

The theory of MIMO radar with randomly positioned elements in the presence of a single target was developed in [4]. The basic idea is to model the locations of the array elements as random, entailing that sidelobes $\left|\mathbf{a}^H(\theta_1)\mathbf{a}\left(\phi_g\right)\right|$ associated with a target at θ_1 and an array beamformed at ϕ_g, with $\phi_g \neq \theta_1$, are also random variables. It is shown that for a sufficiently large number of array elements M, N, a sidelobe $\mathbf{a}^H(\theta_1)\mathbf{a}\left(\phi_g\right)$ has a complex Gaussian distribution. Sidelobes are, in effect, correlated values of $\mathbf{a}^H(\theta_1)\mathbf{a}\left(\phi_g\right)$ viewed as a function of ϕ_g. It can be shown that for a MIMO array, the number of independent sidelobes is approximately $n = 2(Z_T + Z_R)/\lambda$, i.e., the number of sidelobes is proportional to the array effective aperture (sum of the transmit and receive apertures). The 3dB beamwidth of the MIMO array is approximately $\lambda/(Z_T + Z_R)$ rad. Since, (4) relates to K targets, the random array MIMO radar theory for a single target in [4] needs to be extended to multiple targets. We are asking: what are the number of transmit and receive elements required to control the peak sidelobe values when K targets are present, i.e., characterize the statistical properties of $\max_{\phi_g \notin \boldsymbol{\theta}} \left|\sum_{k=1}^K x_k \mathbf{a}^H(\theta_k)\mathbf{a}\left(\phi_g\right)\right|$ parameterized by M and N. Following the approach in [4], it can be shown that $\left|\sum_{k=1}^K x_k \mathbf{a}^H(\theta_k)\mathbf{a}\left(\phi_g\right)\right|$, for $\phi_g \notin \boldsymbol{\theta}$, is Rayleigh distributed with variance $\left(\sum_{k=1}^K |x_k|^2\right)/MN$. From this, the statistics of $\max_{\phi_g \notin \boldsymbol{\theta}} \left|\sum_{k=1}^K x_k \mathbf{a}^H(\theta_k)\mathbf{a}\left(\phi_g\right)\right|$ can be determined. Turning now to the denominator of (4), if targets at θ_j and θ_k are separated by at least one beamwidth (i.e., $\min_{k\neq j} |\theta_k - \theta_j| \geq \lambda/(Z_T + Z_R)$ rad), $\left|\sum_{j\neq k} x_j \mathbf{a}^H(\theta_j)\mathbf{a}(\theta_k)\right|$ is Rayleigh distributed with variance $\left(\sum_{j\neq k} |x_j|^2\right)/MN$, such that $\max_k \left(|x_k| - \left|\sum_{j\neq k} x_j \mathbf{a}^H(\theta_j)\mathbf{a}(\theta_k)\right|\right) \approx \max_k |x_k|$. Finally, letting $|x_k| = 1\ \forall k$, and following a line similar to [4], it can be shown that the number of MIMO radar elements required to guarantee that the peak sidelobe condition (4) is met with probability greater than $1-\gamma$ is

$$MN \geq K \ln \frac{n}{\gamma} \tag{5}$$

Condition (4) (and consequently (5)) refers to the first step of the OLS algorithm. Given a correct decision at that step (say θ_1), the OLS algorithm projects the received vector and the dictionary on the null-space of the steering vector $\mathbf{a}(\theta_1)$. The new received vector is $\sum_{k=2}^K \mathbf{a}(\theta_k) x_k$. New sidelobes $\left|\sum_{k=2}^K x_k \mathbf{a}^H(\theta_k)\mathbf{a}\left(\phi_g\right)\right|$, for $\phi_g \neq \{\theta_k\}_{k=2}^K$, are Rayleigh distributed with a *lower* variance $\left(\sum_{k=2}^K |x_k|^2\right)/MN$ than for the earlier case of K targets. Intuitively, we have removed the interference to the other targets from the first estimated target. Thus, as long as the new denominator $\max_{\phi_g \in \boldsymbol{\theta}} \left|\sum_{k=2}^K x_k \mathbf{a}^H(\theta_k)\mathbf{a}\left(\phi_g\right)\right| \approx \max_{k\in\{2,\ldots,K\}} |x_k|$, the correct recovery of the next target imposes a looser bound, i.e., $MN \geq (K-1)\ln\frac{n}{\gamma}$, guaranteed by (5). In the next section we detail the proposed algorithm enhancing the OLS algorithm by employing global methods.

IV. Problem Solution

In this section, we detail the proposed algorithm, called truncated BB, to address the sparse noisy recovery (3). In particular, assuming K is known, it follows a global optimization approach to solve

$$\min_{\mathbf{x}} \|\mathbf{y} - \mathbf{A}\mathbf{x}\|_2^2 \ \text{ s.t. } \ \|\mathbf{x}\|_0 \leq K \tag{6}$$

The algorithm builds a binary tree where each node is described by a support S and a set $\bar{S}$ of vacant indices, and the tree eventually incorporates all the feasible sets of indices ($|S| \leq K$). The algorithm iteratively explores the tree's leaf nodes (i.e., which have not been split already), until the termination criterion is met. It then returns the support of the minimal norm $\|\mathbf{y} - \mathbf{A}\mathbf{x}\|_2^2$ solution found so far, which correspond to the estimated targets' locations. Since, the first K steps of the proposed algorithm results equivalent to the OLS algorithm, the bound of Sec. III holds for the proposed algorithm as well. The pseudocode of the algorithm is outlined in the following table.

Computational Complexity

Given the $NM \times G$ matrix $\mathbf{A}$, the complexity of the algorithm is closely related to that of OLS, which requires $\mathcal{O}(NMGK)$ multiplications [17]. The truncated BB algorithm with maximum iterations $IterBB$ has complexity $\mathcal{O}(NMG[IterBB])$, which should be compared with the exponential complexity exhaustive search which requires $\mathcal{O}\left(NMG^K K^2\right)$ multiplications. By properly selecting $IterBB$ we can efficiently trade between complexity and performances, as investigated in the next section.

V. Numerical Results

In this section, we present numerical results that demonstrate the potential of global methods for the target localization

Algorithm 1 - Truncated BB

Input: $\mathbf{y}$, $\mathbf{A}$, K and $IterBB$

Output: Support S^* of solution to (6)

Tag root node with $S = \emptyset$ and $\bar{S} = \{1, \ldots, G\}$

Set $Iter = 0$

while $Iter < IterBB$

  Among leaf nodes with $|S| < K$ and max. $\left|S \cup \bar{S}\right|$ select one having max. residual norm $\left\|\Pi^{\perp}_{\mathbf{A}_S}\mathbf{y}\right\|_2$

  Find a $j \in \arg\max_{g \in \bar{S}} \frac{\left\|\mathbf{y}^H \Pi^{\perp}_{\mathbf{A}_S}\mathbf{a}_g\right\|_2}{\left\|\Pi^{\perp}_{\mathbf{A}_S}\mathbf{a}_g\right\|_2}$

  Tag a child node with $S_1 = S \cup j$ and $\bar{S}_1 = \bar{S} \setminus j$

  Tag the other with $S_2 = S$ and $\bar{S}_2 = \bar{S} \setminus j$

  Set $Iter = Iter + 1$

end

Return $S^* \in \arg\min_S \left\|\Pi^{\perp}_{\mathbf{A}_S}\mathbf{y}\right\|_2$

problem. We assume that the receiver knows the number of targets K. The target complex response is selected to have modulo 1 and random phase, uncorrelated between the targets. The MIMO radar transmits orthogonal spread spectrum waveforms of length $L = 10$. The waveforms were chosen as the first M rows of the $L \times L$ Fourier matrix. Equal length apertures were assumed for the transmit and receive arrays, $Z_T = Z_R = 50\lambda$. To ensure the aperture length, elements are placed at locations 0 and 50λ of both the transmit and receive arrays. The locations of the remaining sensors are drawn uniformly at random. We implement target localization using the truncated BB, and several CS techniques: OLS, OMP [18], CSRecSP [19], AIHT [20] and JLZA [21]. In addition, we compare the random array configuration with a MIMO radar geometry which result in a "virtual ULA": the receive elements are $\lambda/2$-spaced, while the transmit elements are $N\lambda/2$-spaced. In the figures, two setting are considered: one (labeled "ULA") with the same number of tx/rx sensors of the random array, but smaller aperture, and one (labeled "Nyquist ULA") with the same virtual array aperture of the random array, but many more sensors (5 tx and 21 rx). For both the "virtual ULA" cases, we include results obtained with the grid-free ESPRIT algorithm [22], where spatial smoothing [23] is employed in order to obtain a covariance matrix of rank K. In each figure, we perform 10000 Monte Carlo realizations varying the target's responses ($x_k = \exp(-j\varphi_k)$ with $\varphi_k \sim \mathcal{U}(0, 2\pi)\ \forall k$), the noise ($\mathrm{vec}(\mathbf{N}) \sim \mathcal{CN}\left(\mathbf{0}, \sigma^2\mathbf{I}\right)$ with $\sigma^2 = 10^{-3}$) and the random array sensors' position. Moreover, since targets' locations are fixed, we linearly spaced grid-points between $-80^\circ + \varepsilon$ and $80^\circ + \varepsilon$, where $\varepsilon \sim \mathcal{U}(-80/G, 80/G)$ is randomized throughout the Monte Carlo realizations. The choice of G is related to the random array resolution ($\simeq 0.6^\circ$): we place 4 grid-points per lobe, i.e., $G = 4 \cdot 160/0.6 \simeq 1001$. The same grid is used for all the recovery methods. As a measure of estimation accuracy, for each realization, we collect the largest modulo of the targets' estimation error, i.e., $\left\|\hat{\boldsymbol{\theta}} - \boldsymbol{\theta}\right\|_\infty \triangleq \max_k \left|\hat{\theta}_k - \theta_k\right|$. We then plot the complementary cumulative distribution function

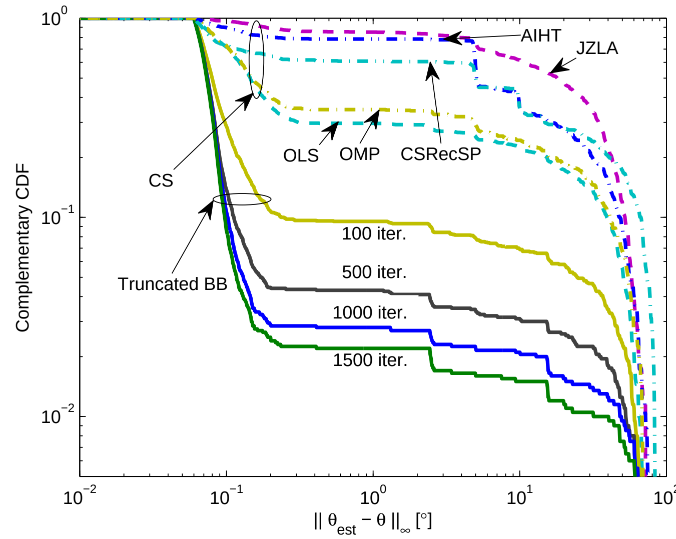

Fig. 1. CCDFs of the truncated BB algorithm with different termination criteria.

(CCDF), defined as $C(x) \triangleq \Pr(X \geq x) = 1 - F(x)$, where F is the cumulative distribution function. The function C is the probability of having an error *greater* then the abscissa, such that a good technique shifts the CCDF towards the bottom-left of the figure. This choice highlights both the resolution and the probability of ambiguities (sidelobes) of each technique.

Fig. 1 plots the CCDFs of the recovery error for various levels of truncation of the BB algorithm (100, 500, 1000, 1500 iterations), and compares it with the performance of several CS techniques. The system settings are $M = N = 5$ and $K = 4$ targets at $\boldsymbol{\theta} = [-7.5^\circ, -2.5^\circ, 2.5^\circ, 7.5^\circ]$. It can be seen how with only 100 iterations we obtain considerable better performance then with the conventional CS methods. Moreover, limiting the iterations to 1000, the error drops to almost 5%, and it continues to diminish as the iterations are increased to 1500.

Fig. 2, plots the CCDFs for the random array and the ULA for various algorithms: truncated BB, OLS, as well as ESPRIT in the two ULA setting. The system settings are $M = N = 5$, $K = 2$ targets at $\boldsymbol{\theta} = [-2.5^\circ, 2.5^\circ]$, and the BB algorithm is terminated after 1000 iterations. It is observed that OLS and ESPRIT perform poorly in the ULA scenario. This is explained by the smaller aperture of the ULA (10λ) compared to that of the random array (50λ). The BB algorithm achieves high performance for both array geometries: it considerably improves the performance of the ULA case, while, in the random array scenario, by exploiting the system's higher resolution, it further improves performance maintaining the probability of a localization error larger than 0.1° lower than 10^{-4}. Moreover, the truncated BB is only slightly worse then the ESPRIT in the Nyquist ULA system, enforcing the spatial CS paradigm.

Finally, in Fig. 3, we investigate performance as a function of the number of transmit/receive elements of the MIMO radar. It is observed that the localization error decreases with the

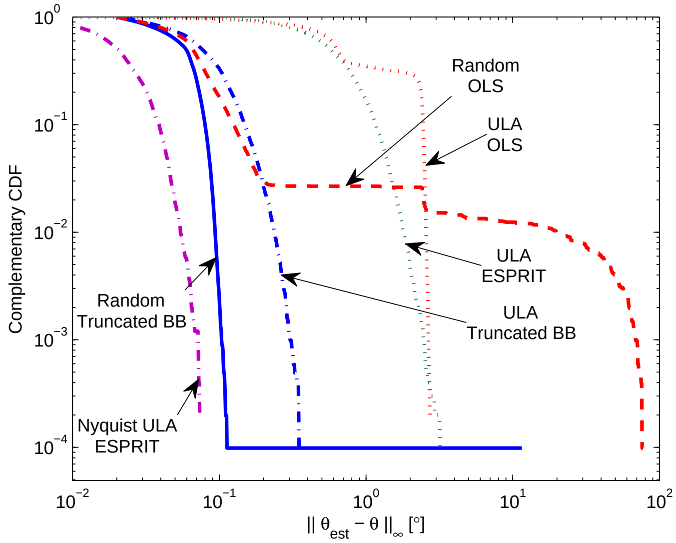

Fig. 2. CCDFs for random array and ULA with the truncated BB, OLS, JLZA, and ESPRIT algorithms.

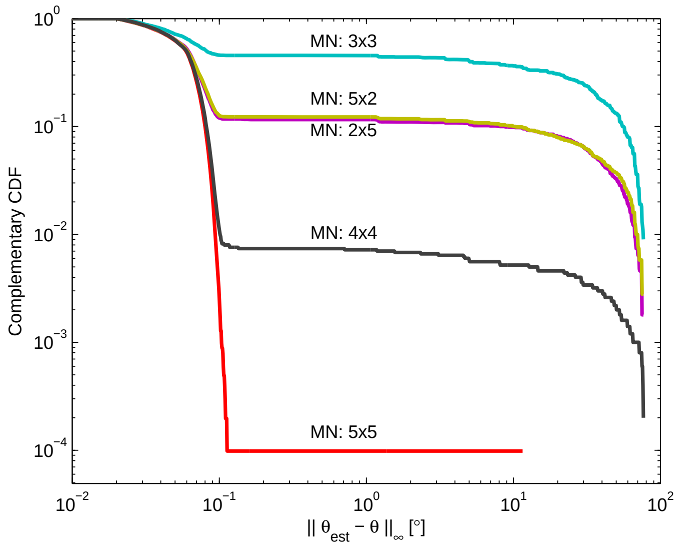

Fig. 3. CCDFs for the truncated BB algorithm parametrized by the number of transmit/receive elements.

increase of the MN product. According to (5), for $K = 2$ targets, a dictionary of $G = 1001$ atoms, and a probability of error smaller than of 10^{-3}, the number of elements required should meet $MN \geq 2 \cdot \ln\left(\frac{2}{\lambda}\left[Z_T + Z_R\right]/10^{-3}\right) \approx 24$. This relation is corroborated by the figure, where with fewer elements the error increases (e.g., the localization error has probability of 10^{-1} with $MN = 10$), whereas the probability of error decreases with a larger number of elements (e.g., the localization error has probability 10^{-4} with $MN = 25$).

VI. Conclusions

We address the source localization problem in MIMO radar by using a sparse representation framework. We develop a global method algorithm for the sparse recovery problem and we derive an explicit lower bound on the number of random array elements needed to achieve a target probability of correct DOA estimation. The lower bound provides specific insight into links between random arrays and CS algorithms, and demonstrates that a high resolution can be obtained with a relatively low number of randomly placed sensors.

References

[1] A. M. Haimovich, R. Blum, and L. Cimini, “MIMO radar with widely separated antennas,” IEEE Sig. Proc. Mag., vol.25, no.1, pp.116–129, 2008.

[2] C.-Y. Chen and P.P. Vaidyanathan, “MIMO Radar Space-Time Adaptive Processing Using Prolate Spheroidal Wave Functions,” IEEE Trans. Sig. Proc., vol.56, no.2, pp.623–635, Feb. 2008.

[3] Y. Lo, “A mathematical theory of antenna arrays with randomly spaced elements,” IEEE Trans. on Antennas and Propagation, vol.12, no.3, pp.257–268, May 1964.

[4] M. A. Haleem and A. M. Haimovich, “On the distribution of ambiguity levels in MIMO radar,” Proc. 42nd Asilomar Conf. on Signals, Systems and Computers, Pacific Grove, CA, Oct. 2008.

[5] D. Donoho, “Compressed sensing,” IEEE Trans. on Information Theory, vol.52, no.4, pp. 1289–1306, 2006.

[6] S. Chen, S. A. Billings, and W. Luo, “Orthogonal least squares methods and their application to non-linear system identification,” Int. Journal of Control, vol.50, no.5, pp.1873–1896, 1989.

[7] E. J. Candes and M.B. Wakin, “An Introduction To Compressive Sampling,” IEEE Sig. Proc. Mag., vol.25, no.2, pp.21–30, Mar. 2008.

[8] R. Chartrand, “Exact reconstruction of sparse signals via nonconvex minimization,” IEEE Sig. Proc. Lett., vol.14, pp.707–710, Oct. 2007.

[9] K. Gedalyahu and Y. C. Eldar, "Time-Delay Estimation From Low-Rate Samples: A Union of Subspaces Approach", IEEE Trans. Sig. Proc., vol.58, no.6, pp.3017–3031, Jun. 2010.

[10] W. U. Bajwa, K. Gedalyahu, and Y. C. Eldar, “Identification of parametric underspread linear systems with application to super-resolution radar,” IEEE Trans. Sig. Proc., vol.59, no.6, pp.2548–2561, Aug. 2011.

[11] M. Herman and T. Strohmer, “Compressed Sensing Radar,” Proc. IEEE Int. Conf. Acoust., Speech Sig. Proc., Mar 2008.

[12] D. Malioutov, M. Cetin, and A. S. Willsky, “A sparse signal reconstruction perspective for source localization with sensor arrays,” IEEE Trans. Sig. Proc., vol.53, no.8, pp.3010–3022, 2005.

[13] T. Strohmer and B. Friedlander, “Compressed sensing for MIMO radar - algorithms and performance,” Proc. 43rd Asilomar Conf. on Signals, Systems and Computers, Pacific Grove, CA, Nov. 2009.

[14] L. Carin, “On the relationship between compressive sensing and random sensor arrays,” IEEE Ant. Prop. Mag., vol.5, no.5, pp.72–81, Oct. 2009.

[15] J. H. G. Ender, “On compressive sensing applied to radar,” Signal Process, vol.90, pp.1402–1414, 2010.

[16] Y. Yu, A. P. Petropulu, and H. V. Poor, “MIMO Radar Using Compressive Sampling ,” IEEE J. Sel. Topics in Sig. Proc., vol.4, no.1, pp.146–163, Feb. 2010.

[17] E. S. Chng, S. Chen, and B. Mulgrew, “Efficient computational schemes for the orthogonal least squares algorithm,” IEEE Trans. Sig. Proc., vol.43, no.1, pp.373–376, 1995.

[18] Y. C. Pati, R. Rezaifar, and P. S. Krishnaprasad, “Orthogonal matching pursuit: recursive function approximation with applications to wavelet decomposition,” Proc. 27th Asilomar Conf. on Signals, Systems and Computrs, Nov. 1993.

[19] W. Dai and O. Milenkovic, “Subspace pursuit for compressive sensing signal reconstruction,” IEEE Trans. Inf. Theory, vol.55, no.5, pp.2230–2249, 2009.

[20] T. Blumensath, “Accelerated Iterative Hard Thresholding,” availble at: *users.fmrib.ox.ac.uk/~tblumens/papers/B_AIHT.pdf*, unpublished.

[21] M. M. Hyder and K. Mahata, “A joint sparse signal representation perspective for target detection using bistatic MIMO radar system,” Proc. of 17th Int. Conf. on DSP, 6-8 July 2011.

[22] R. Roy and T. Kailath, “ESPRIT-estimation of signal parameters via rotational invariance techniques,” IEEE Trans. Acoust., Speech, Sig. Proc., vol.37, no.7, pp.984–995, Jul. 1989.

[23] T.-J. Shan, M. Wax, and T. Kailath, “On spatial smoothing for direction-of-arrival estimation of coherent signals,” IEEE Trans. Acoust., Speech, Sig. Proc., vol.33, no.4, pp.806–811, Aug. 1985.